Structure and properties of spin-coated $Ge_{25}S_{75}$ chalcogenide thin films

Stanislav Slang[1], Petr Janicek[2,1], Karel Palka[3,1,*], and Miroslav Vlcek[1]

[1]*Center of Materials and Nanotechnologies, Faculty of Chemical Technology, University of Pardubice, Studentska 95, Pardubice 532 10, Czech Republic*
[2]*Institute of Applied Physics and Mathematics, Faculty of Chemical Technology, University of Pardubice, Studentska 95, Pardubice 532 10, Czech Republic*
[3]*Department of General and Inorganic Chemistry, Faculty of Chemical Technology, University of Pardubice, Studentska 95, Pardubice 532 10, Czech Republic*
[*]*karel.palka@upce.cz*

Abstract: Amorphous chalcogenide thin films of $Ge_{25}S_{75}$ composition have been deposited by spin-coating technique. Optical properties of thin films were investigated by spectroscopic ellipsometry in UV-MIR spectral range. Obtained results prove increase of thin films refractive index in the transparent region and decrease of their thickness with increasing annealing temperature implying densification of the glass structure. Short wavelength absorption edge is shifting to lower energies (red shift) with increasing annealing temperature. Decreasing organic molecules content with increasing temperature of annealing was observed in MIR part of extinction coefficient and verified by Raman spectroscopy and EDS. Raman spectra also gave evidence of thermo-induced structural polymerization and decomposition of organic salts molecules yielding thin films with structure similar to the structure of the source bulk glass.

Keywords: (160.2750) Glass and other amorphous materials; (310.6860) Thin films, optical properties; (310.6870) Thin films, other properties; (240.2130) Ellipsometry and polarimetry.

References and links

1. A. Stronski, M. Vlcek, and A. Sklenar, "Image formation properties of As-S thin layers," Quant. Electron. Optoelectron **3**(3), 394–399 (2000).
2. A. Zoubir, M. Richardson, C. Rivero, A. Schulte, C. Lopez, K. Richardson, N. Hô, and R. Vallee, "Direct femtosecond laser writing of waveguides in As_2S_3 thin films," Opt. Lett. **29**(7), 748–750 (2004).
3. S. Song, S. S. Howard, Z. Liu, A. O. Dirisu, C. F. Gmachl, and C. B. Arnold, "Mode tuning of quantum cascade lasers through optical processing of chalcogenide glass claddings," Appl. Phys. Lett. **89**, 041115 (2006).
4. G. Lucovsky and J. Philips, "Reversible chemical phase separation in on-state of art ReWritable (RW) $Ge_2Sb_2Te_5$ optical phase change memories," J. Non-Cryst. Solids **354**(19–25), 2753–2756 (2008).
5. A. Abrutis, V. Plausinaitiene, M. Skapas, C. Wiemer, O. Salicio, M. Longo, A. Pirovano, J. Siegel, W. Gawelda, S. Rushworth, and C. Giesen, "Chemical vapor deposition of chalcogenide materials for phase-change memories," Microelectron. Eng. **85**(12), 2338–2341 (2008).
6. H. Jain and M. Vlcek, "Glasses for lithography," J. Non-Cryst. Solids **354**, 1401–1406 (2008).
7. V. A. Dan'ko, I. Z. Indutnyi, V. I. Min'ko, P. E. Shepelyavyi, O. V. Bereznyova, and O. S. Lytvyn, "Photoinduced etching of thin films of chalcogenide glassy semiconductors," Semiconductors **46**(4), 504–508 (2012).
8. Y. Chen, X. Shen, R. Wang, G. Wang, S. Dai, T. Xu, and Q. Nie, "Optical and structural properties of Ge–Sb–Se thin films fabricated by sputtering and thermal evaporation," J. Alloy. Compd. **548**, 155–160 (2013).
9. A. V. Rode, A. Zakery, M. Samoc, R. P. Charters, E. G. Gamaly, and B. Luther- Davies, "Laser-deposited As_2S_3 chalcogenide films for waveguide applications," Appl. Surf. Sci. **197–198**, 481–485 (2002).
10. T. Kanamori, Y. Terunuma, S. Takahashi, and T. Miyashita, "Chalcogenide glass fibers for midinfrared transmission," J. Lightwave Technol. **2**, 607 (1984).
11. K. Tanaka and M.. Mikami, "Photoinduced vector deformations of semi-freely ixed glassy As-S(Se)," Phys. Status Solidi C **8**, 2756–2760 (2011).
12. G. C. Chern and I. Lauks, "Spin coated amorphous chalcogenide films," J. Appl. Phys. **53**(10), 6979–6982 (1982).
13. G. C. Chern, I. Lauks, and A. R. McGhie, "Spin coated amorphous chalcogenide films: Thermal properties," J. Appl. Phys. **54**(8), 4596–4601 (1983).

14. S. A. Zenkin, S. B. Mamedov, M. D. Mikhailov, E. Yu. Turkina, and I. Yu. Yusupov, "Mechanism for Interaction of Amine solutions with Monolythic Glasses and Amorphous Films in the As–S System," Glass Phys. Chem. **23**(5), 393–399 (1997).
15. Y. Zha, M. Waldmann, and C. B. Arnold, "A review on solution processing of chalcogenide glasses for optical components," Opt. Mater. Express **3**(9), 1259–1272 (2013).
16. S. Slang, K. Palka, L. Loghina, A. Kovalskiy, H. Jain, and M. Vlcek, "Mechanism of the dissolution of As–S chalcogenide glass in n-butylamine and its influence on the structure of spin coated layers," J. Non-Cryst. Solids **426**, 125–131 (2015).
17. J. Cook, S. Slang, R. Golovchak, H. Jain, M. Vlcek, and A. Kovalskiy, "Structural features of spin-coated thin films of binary As_xS_{100-x} chalcogenide glass system," Thin Solid Films **589**, 642–648 (2015).
18. K. Palka, T. Syrovy, S. Schröter, S. Brückner, M. Rothhardt, and M. Vlcek, "Preparation of arsenic sulfide thin films for integrated optical elements by spiral bar coating," Opt. Mater. Express **4**(2), 384–395 (2014).
19. S. Novak, D. E. Johnston, Ch. Li, W. Deng, and K. Richardson, "Deposition of $Ge_{23}Sb_7S_{70}$ chalcogenide glass films by electrospray," Thin Solid Films **588**, 56–60 (2015).
20. S. Song, N. Carlie, J. Boundies, L. Petit, K. Richardson, and C. B. Arnold, "Spin-coating of $Ge_{23}Sb_7S_{70}$ chalcogenide glass thin films," J. Non-Cryst. Solids **355**, 2272–2278 (2009).
21. L. Loghina, K. Palka, J. Buzek, S. Slang, and M. Vlcek, "Selective wet etching of amorphous As_2Se_3 thin films," J. Non-Cryst. Solids **430**, 21–24 (2015).
22. D. A. G. Bruggeman, "Berechnung verschiedener physikalischer Konstanten von heterogenen substanzen," Ann. Phys. (Leipzig) **24**, 636–679 (1935).
23. G.E. Jellison Jr. and F.A. Modine, "Parametrization of the optical functions of amorphous materials in the interband region," Appl. Phys. Lett. **69**, 371–373 (1996), Erratum, Appl. Phys. Lett. **69**, 2137–2139 (1996).
24. Y. Zou, H. Lin, O. Ogbuu, L. Li, S. Danto, S. Novak, J. Novak, J. D. Musgraves, K. Richardson, and J. Hu, "Effect of annealing conditions on the physio-chemical properties of spin-coated As_2Se_3 chalcogenide glass films," Opt. Mater. Express **2**(12), 1723–1732 (2012).
25. S. Song, J. Dua, and C. B. Arnold, "Influence of annealing conditions on the optical and structural properties of spin-coated As_2S_3 chalcogenide glass thin films," Opt. Express **18**(6), 5472–5480 (2010).
26. T. S. Moss, *Photoconductivity in the Elements*, Butterworths Sci. Pubi., London, 1952.
27. T. S. Moss, *Optical Properties of Semiconductors*, Butterworths Sci. Pubi., London, 1959.
28. P. Taheri, H. Terryn, and J. Mol, "An in situ study of amine and amide molecular interaction on Fe surfaces," Appl. Surf. Sci. **354**, 242–249 (2015).
29. G. Shustak, A.J. Domb, and D. Mandler, "Preparation and characterization of n-alkanoic acid self-assembled monolayers adsorbed on 316L stainless steel," Langmuir **20**, 7499–7506 (2004).
30. Y.T. Tao, "Structural comparison of self-assembled monolayers of n-alkanoic acids on the surfaces of silver, copper, and aluminum," J. Am. Chem. Soc. **115**(10), 4350–4358 (1993).
31. H. Behniafar, M. Alimohammadi, and K. Malekshahinezhad, "Transparent and flexible films of new segmented polyurethane nanocomposites incorporated by NH_2-functionalized TiO_2 nanoparticles," Prog. Org. Coat. **88**, 150–154 (2015).
32. L. J. Bellamy, *The infrared spectra of complex molecules*, John Wiley & Sons, New York, 1975.
33. Y. Liu, G.J. Zhang, S.Q. Sun, and I. Noda, "Study on similar traditional Chinese medicines cornu Cervi pantotrichum, cornu Cervi and cornu Cervi degelatinatum by FT-IR and 2D-IR correlation spectroscopy," J. Pharm. Biomed. Anal. **52**, 631–635 (2010).
34. K. Choong, J. Lan, H. Lee, X. Chen, X. Wang, and Y. Yang, "Differential identification of mushrooms sclerotia by IR macro-fingerprint method," Spectrochim. Acta A **152**, 34–42 (2016).
35. K. Tanaka and M. Yamaguchi, "Resonant Raman scattering in GeS_2," J. Non-Cryst. Solids **227–230**, 757–760 (1998).
36. H. Guo, H. Tao, Y. Zhai, S. Mao, and X. Zaho, "Raman spectroscopic analysis of GeS_2–Ga_2S_3–PbI_2 chalcohalide glasses," Spectrochim. Acta A **67**, 1351–1356 (2007).
37. T. Haizheng, Z. Xiujiang, and J. Chengbin, "Raman spectroscopic study on the microstructure of GeS_2–Ga_2S_3–KCl glasses," J. Mol. Struct. **697**, 23–27 (2004).
38. Z. Cernosek, E. Cernoskova, and L. Benes, "Raman scattering in GeS_2 glass and its crystalline polymorphs compared," J. Mol. Struct. **435**, 193–198 (1997).
39. T. Cardinal, K. A. Richardson, H. Shim, A. Schulte, R. Beatty, k. Le Foulgoc, C. Meneghini, J. F. Viens, and A. Villeniuve, "Non-linear optical properties of chalcogenide glasses in the system As-S-Se," J. Non-Cryst. Solids **256&257**, 353–360 (1999).
40. M. Pisarcik and L. Koudelka, "Raman Spectra and Structure of Germanium-Arsenic-Sulfur Glasses in the Sulfur-Rich Region," Mater. Chem. **7**, 499–507 (1982).
41. Z. Cernosek, J. Holubova, E. Cernoskova, and A. Ruzicka, "Sulfur – a new information on this seemingly well-known element," J. Non-oxide Glas. **1**(1), 38– 42 (2009).

1. Introduction

Chalcogenide glasses (ChGs) are promising semiconductor optical materials exhibiting high values of refractive index and wide IR transparency. They have found applications in VIS and IR optics (diffractive optical elements, waveguides and others [1–3]), optical memories [4, 5] and also as high resolution photoresists [6, 7]. Thin films of ChGs are usually deposited by vacuum based deposition techniques, such as vacuum thermal evaporation, sputtering or laser ablation [1–9]. Thin films deposited by these techniques usually have significantly more disordered structure in comparison with those of source bulk ChG often resulting in photosensitivity of thin films [10, 11]. Deposition of thin films is relatively expensive due to the necessity of high vacuum equipment.

Alternatively, thin films of ChGs can be deposited by solution based deposition techniques exploiting the fact that ChGs can be dissolved in volatile organic bases. Spin-coating and dip-coating deposition methods are frequently used for ChG thin films deposition [12–17], but these techniques are suitable only for basic material research and small scale production. Well known and managed printing [18] and coating [19] techniques allowing continuous deposition are gaining attention for large scale production purposes.

Solution based deposition techniques allow good films composition control, which can be often challenging in case of some vacuum based deposition methods such as thermal evaporation. Because the solution based depositions are usually carried out under normal pressure the production is significantly cheaper as there is no need for high vacuum equipment. Major disadvantage of solution based deposition methods are the residual amount of solvent remaining in the thin film's structure. But its content can be significantly lowered by proper annealing [12, 13, 16].

Thin films deposited by solution based techniques have been widely studied on arsenic-based ChGs [12–17], which limits their wide-spread application due to the arsenic toxicity. Germanium-based spin-coated thin films of $Ge_{23}Sb_7S_{70}$ glass composition were successfully prepared [20], but further study of other germanium-based systems is needed to obtain plurality of different non-toxic optical materials prepared by solution based deposition techniques.

In this paper, we present a study of non-toxic $Ge_{25}S_{75}$ thin films prepared by spin-coating method with specular optical quality. The influence of annealing treatment on films properties is reported. Optical parameters and thickness of studied thin films were determined by spectroscopic ellipsometry (SE). Structural changes and residual organics content were studied by Raman spectroscopy and energy-dispersive x-ray spectroscopy (EDS). Thermo-induced structural polymerization mechanism was proposed based on experimental findings.

2. Experiment

The source bulk $Ge_{25}S_{75}$ ChG was prepared by standard melt-quenching method. High purity (5N) elements were loaded into the quartz ampule in appropriate amounts and sealed under vacuum (~10^{-3} Pa). The glass synthesis was performed in rocking tube furnace at 950 °C for 72 hours. The ampule with melted glass was quenched in cold water.

Prepared bulk glass was grinded in agate bowel and dissolved in n-butylamine (BA) with concentration 0,075 g of glass powder per 1 ml of BA solvent. The thin films were deposited using spin-coating method (spin-coater Best Tools SC110) onto soda-lime glass substrates yielding thin films of good optical quality. Immediately after deposition the thin films were stabilized by annealing at 60 °C for 20 minutes on a hot plate (hereinafter referred as as-prepared thin film). Deposited samples were stored in dry and dark environment.

Samples of as-prepared thin films were annealed at temperatures 90, 120, 150, 180 and 210 °C for 60 minutes on annealing table (Conbrio, Czech Republic) inside argon filled annealing chamber.

Two variable angle spectroscopic ellipsometers (VASE and IR-VASE J. A. Woollam Co.) were used for the optical characterization of the prepared samples. The first ellipsometer was equipped with an automatic rotating analyzer over the spectral range 210 nm – 1700 nm (UV-VIS-NIR), measuring 30 revolutions with photon energy steps of 0.05 eV at three

selected angles of incidence (AOI) (50°, 60° and 70°). The second ellipsometer was equipped with a rotating compensator for 1.7 – 22 μm (NIR-MIR), using same AOI, measuring 25 scans, 15 spectra per revolution with wavenumber steps 8 cm^{-1}. Near normal incidence optical reflectance was measured by the same instruments. Optical spectrometer (Shimadzu UV3600) was used for transmission spectra measurements in the spectral region 190 – 2000 nm. WVASE32 software was used for evaluation the measured data.

Surface topography of spin-coated $Ge_{25}S_{75}$ thin films was studied by atomic force microscopy method (Solver NEXT, NT-MDT). Surface roughness was determined from measured data as a root mean square value (RMS) according to the ISO 4287/1 norm. The measurements were performed on two 10 x 10 μm spots of the same thin film and obtained RMS values were averaged.

The as-prepared and annealed thin films were analyzed by energy dispersion x-ray microanalysis method using scanning electron microscope (LYRA 3, Tescan) equipped with EDS analyzer Aztec X-Max 20 (Oxford Instruments) at acceleration voltage 5 keV. The etching kinetics of as-prepared and annealed thin film samples were studied by procedure presented in [21] in 0.1% vol. BA solution in aprotic solvent. The etching curves were evaluated at two wavelengths corresponding to the first interference maximum and the first minimum of measured transmission spectra.

The structure of source bulk glass, spin-coated thin films and pure BA solvent was determined using FT IR spectrometer IFS55 equipped with Raman module FRA106 (Bruker) with excitation by Nd:YAG laser (1064 nm). Raman spectra were measured with laser beam intensity of 120 mW (2 cm^{-1} resolution, 200 scans). The Raman spectra were normalized by intensity of the most intense band in the spectrum.

3. Results and Discussion

Spin-coated thin films deposited onto microscopic soda-lime glass slides were investigated using spectroscopic ellipsometry (SE). The change of the polarization state is usually expressed by two parameters, amplitude ratio ψ and phase shift Δ, that are defined using the Fresnel reflection coefficients for p- and s- polarized light:

$$\frac{r_p}{r_s} = tan(\psi) \cdot e^{(i\Delta)}. \tag{1}$$

SE is an indirect optical characterization method, where the measured values ψ^{exp} and Δ^{exp} are compared to the values calculated from the model. In the model structure, the optical constants of the films and their thicknesses are assumed, and it is possible to calculate the corresponding values of ψ^{mod} and Δ^{mod} belonging to the proposed model structure. Geometrical properties, such as thickness of the film and surface roughness, could also be determined as parameters of the model. In this way, the optical parameters of studied films, such as complex refractive index (which includes refractive index as the real part and extinction coefficient as the imaginary part) can be calculated. Computation of various parameters of the films was performed via regression analysis, where the minimization procedure was based on the mean square error (MSE) values; MSE is given in the following expression:

$$MSE = \sqrt{\frac{1}{2N-M}\sum_{i=1}^{N}\left[\left(\frac{\psi_i^{\mathrm{mod}} - \psi_i^{\mathrm{exp}}}{\sigma_{\psi,i}^{\mathrm{exp}}}\right)^2 + \left(\frac{\Delta_i^{\mathrm{mod}} - \Delta_i^{\mathrm{exp}}}{\sigma_{\Delta,i}^{\mathrm{exp}}}\right)^2\right]}, \tag{2}$$

where N is the number of measured pairs of ellipsometric parameters ψ^{exp} and Δ^{exp} and M represents the total number of fitted parameters. $\sigma_{\psi,i}^{\mathrm{exp}}$ and $\sigma_{\Delta,i}^{\mathrm{exp}}$ are then the estimated experimental error of ψ^{exp} and Δ^{exp}, respectively. Ellipsometric data measured for all three angles of incidence 50°, 60° and 70° were used in the fit simultaneously.

The sample model used for ellipsometry spectra analyses consists of: 1) a semi-infinite glass substrate (with optical constants obtained previously on a blank sample of uncoated

microscopic soda-lime glass slide), 2) a homogenous, isotropic film representing the spin-coated $Ge_{25}S_{75}$ thin film annealed at different temperatures, 3) surface roughness modeled by a Bruggeman type effective medium approximation of the voids and layers [22], and 4) air as the ambient medium.

The wide spectral range was split into two parts, where the measured data were processed differently. The UV-VIS-NIR part of the spectrum in the 0.7 – 6 eV (≈ 1.77 μm – 0.2 μm) range was fitted separately from the MIR part of spectra in 0.05 eV – 0.7 eV (≈ 24.8 μm – 1.77 μm).

The short wavelength absorption edge is present in the UV-VIS-NIR part of the spectra of amorphous semiconductors. Tauc-Lorentz oscillator has been used for description of this band edge of studied films. Although more sophisticated (and more complicated) models have been used for description of short wavelength edge of amorphous semiconductors in the literature, Tauc-Lorentz model describes measured data very well (MSE less than 2.3 for all samples) and with only 4 free parameters we consider Tauc-Lorentz oscillator as simple and concurrently sufficient for description of measured data. In order to ensure validity of short wavelength absorption edge determination and thickness of the thin film data from transmission and reflection has been used in the fit together with the ellipsometry data with MSE minimization in similar manner as described by eq. 2. Model dielectric function for Tauc-Lorentz oscillator is given by function [23]:

$$\varepsilon_2 = \frac{A \cdot E_0 \cdot C \cdot \left(E - E_g^{opt}\right)^2}{\left(E^2 - E_0^2\right)^2 + C^2 \cdot E^2} \cdot \frac{1}{E} \qquad for\ E > E_g^{opt}$$

$$\varepsilon_2 = 0 \qquad for\ E \le E_g^{opt} \tag{3}$$

$$\varepsilon_1 = \frac{2}{\pi} P \int_{E_g}^{\infty} \frac{\xi \cdot \varepsilon_2(\xi)}{\xi^2 - E^2} d\xi.$$

In this model, film is transparent below E_g^{opt} (called optical bandgap). This value is usually estimated from so called Tauc plot from transmission measurement. Other used parameters A, E_0, C stand for amplitude, peak position and broadening of the oscillator. Example of measured ellipsometry data together with the best fit by described model for as-prepared sample and angle of incidence 60° is depicted at Fig. 1.

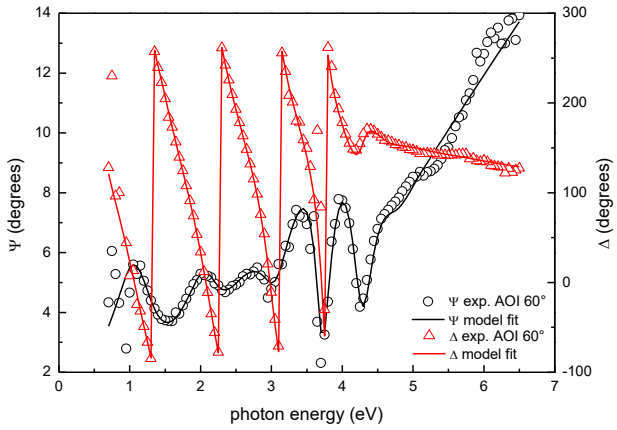

Fig. 1: Measured values of ψ (circles) and Δ (triangles) for UV-VIS part of spectra of as-prepared thin film together with the best fit (solid line) for the angle of incidence 60°.

Geometrical and optical parameters (thickness of the films and surface roughness together with the confidence intervals, optical bandgap and refractive index values at 1550

nm) obtained using this model, are summarized in Table 1. Values of surface roughness determined by SE are in good agreement with AFM data reported in Table 1 as well. The thickness and surface roughness values of studied thin films are also presented in Fig. 2.

Sample	SE thickness (nm)	SE roughness (nm)	AFM roughness (nm)	E_g^{opt} (eV)	n_{1550}
as-prepared	396 ± 0.2	0.3 ± 0.1	0.40 ± 0.13	3.45	1.70
T-90 °C	378 ± 0.2	0.9 ± 0.1	0.69 ± 0.24	3.33	1.70
T-120 °C	345 ± 0.2	2.3 ± 0.1	0.83 ± 0.50	3.17	1.71
T-150 °C	260 ± 0.2	5.5 ± 0.1	7.64 ± 1.02	3.06	1.81
T-180 °C	220 ± 0.2	5.1 ± 0.1	5.36 ± 0.22	3.05	1.88
T-210 °C	197 ± 0.2	11.2 ± 0.1	13.68 ± 0.83	3.04	1.94

Table 1: Values of thin film's thickness, surface roughness (spectroscopic ellipsometry – SE, atomic force microscopy – AFM), optical bandgap (E_g^{opt}) and refractive index values (n_{1550}) for 1550 nm determined by spectroscopic ellipsometry.

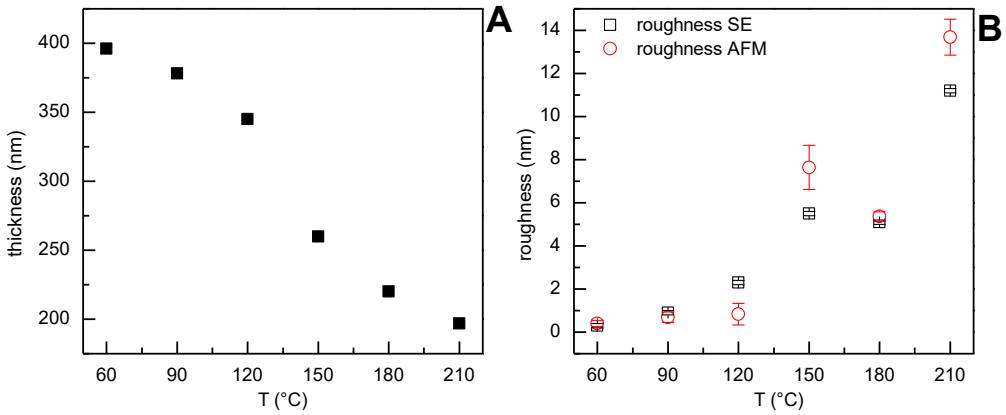

Fig. 2: Thickness (A) and surface roughness (B) of studied thin films obtained from spectroscopic ellipsometry (SE) and atomic force microscopy (AFM) in dependence on the annealing temperature.

Model of Tauc-Lorents oscillator (eq. 3) has been used for all 6 spin-coated samples annealed at different temperatures. Calculated spectral dependences of refractive index, extinction coefficient respectively, are depicted in Fig. 3 and Fig. 4.

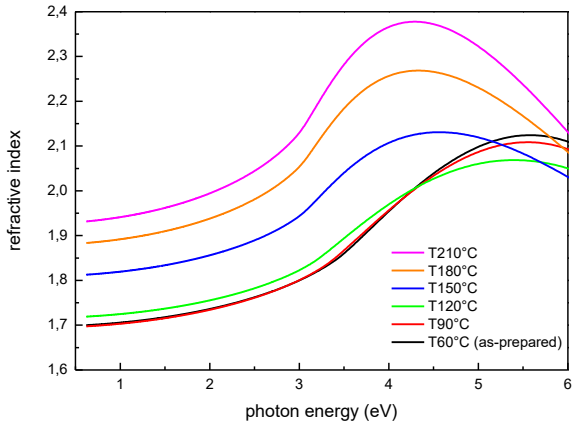

Fig. 3: Calculated refractive index of spin-coated $Ge_{25}S_{75}$ thin films annealed at various temperatures as a function of photon energy in UV-VIS-NIR.

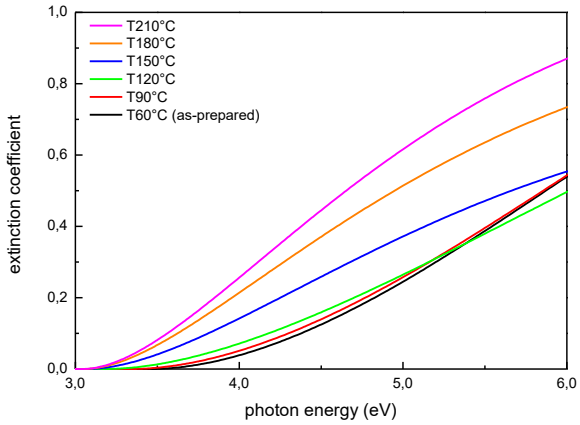

Fig. 4: Calculated extinction coefficient of spin-coated $Ge_{25}S_{75}$ thin films annealed at various temperatures as a function of photon energy in the vicinity of short wavelength absorption edge.

The refractive index in the transparent region of spin-coated $Ge_{25}S_{75}$ thin films is monotonously increasing with the increasing annealing temperature. Observed increase could be explained by increasing compactness of the film (densification). According to [13] the freshly prepared spin-coated thin films of As-S system consist of glass clusters separated by voids and organic molecules used in the solution. The organic molecules are ionically bonded to the ChG clusters in form of alkyl ammonium chalcogenide salt. When annealing process decomposes these salts and subsequently evaporates organics molecules, the glass particles are forming more compact film [15]. This observation has been reported in the literature earlier for spin-coated As_2Se_3 and As_2S_3 films [24, 25]. Similar mechanism can be expected for ChGs of Ge-S system as well, which would be in a good agreement with observed significant decrease of the thin films thickness during the annealing process (Table 1; Fig. 2A).

From spectral dependence of extinction coefficient and consequently from parameter E_g^{opt} of used Tauc-Lorentz oscillator the shift of the short wavelength absorption edge to lower energies (red shift) with the increasing annealing temperature can be observed (see Fig. 4 and Fig. 5). Red shift of absorption edge with increasing annealing temperature has been also observed for spin-coated As_2Se_3 and As_2S_3 glasses consistently with our findings for spin-coated $Ge_{25}S_{75}$ thin films [24, 25]. An increase of the annealing temperature was found to lead to (i) lower thickness, (ii) reduced optical bandgap indicating higher values of static relative permittivity [26, 27], (iii) higher values of refractive index of the film and (iv) increased surface roughness.

The second part of the spectral range, i.e., the MIR part (0.05 eV – 0.7 eV), was fitted using the same 4 layer model used for UV-VIS-NIR part. The thickness was introduced from previous regression analysis of the UV-VIS-NIR part of spectra. Generally amorphous semiconductors should be transparent up to long wavelength absorption edge whose position is determined by absorption of photons on the phonon modes. Due to amorphous nature of studied films sum of gauss oscillators has been used as a model dielectric function for this part of spectra.

To describe measured ellipsometry data totally 5 gauss oscillators with center energies (2900 cm^{-1}, 1520 cm^{-1}, 1180 cm^{-1}, 1000 cm^{-1} and ≈ 440 cm^{-1}) have been used with MSE less than 1.7 for all samples (Fig. 6). Oscillator positioned at ≈ 440 cm^{-1} describes the long wavelength absorption edge and its position is changing. Considering used measurement resolution (8 cm^{-1}) in the MIR part of the spectra the position of long wavelength absorption edge can be determined only approximately.

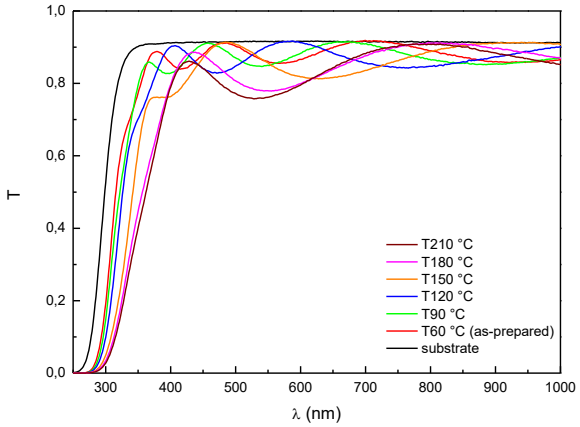

Fig. 5: Measured transmission spectra for spin-coated $Ge_{25}S_{75}$ thin films annealed at different temperatures.

Gauss oscillators at 2900 cm^{-1}, 1520 cm^{-1}, 1180 cm^{-1} and 1000 cm^{-1} maintain the position nearly identical for all studied thin films. These oscillators very likely correspond to vibrations of organic molecules used for spin-coating precursor. The absorption band in MIR with position 2900 cm^{-1} (≈ 3.5 μm) can be attributed to $–CH_2–$, $–CH_3$ and $–NH_2$ vibrations [28–30], 1520 cm^{-1} (≈ 6.6 μm) to $–NH_2$ vibrations [28, 31], 1180 cm^{-1} (≈ 8.5 μm) to R–NH–R vibration [32] and band at 1000 cm^{-1} (≈ 10 μm) to so-called fingerprint area of BA's IR spectrum [33, 34]. The intensity of the band at 2900 cm^{-1} is decreasing significantly with increasing annealing temperature (Fig. 6.). Observed data correspond to increase of compactness of the thin film with increasing annealing temperature, which is with good agreement with data from UV-VIS-NIR SE (Table 1, Fig. 2).

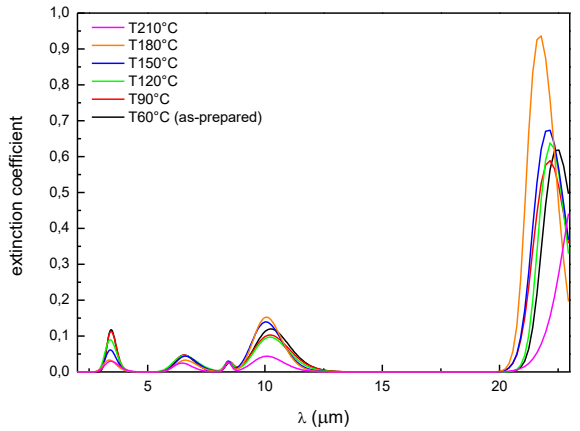

Fig. 6: Calculated extinction coefficient of studied spin-coated $Ge_{25}S_{75}$ thin films annealed at different temperatures as a function of wavelength in MIR part of spectra.

To verify the Ge, S and organic molecules content the EDS measurements were performed for all studied thin film samples. The obtained results proved that Ge_xS_{100-x} atomic ratio slightly changes after annealing of deposited thin films (Fig. 7). The sulfur content gradually decreases with increasing annealing temperature and stabilizes at approx. $Ge_{28}S_{72}$ composition after annealing at and above 150 °C. Observed decrease of sulfur content could be explained by partial evaporation of the sulfur from the surface layer of the thin film during the annealing process due to the overstoichiometry of the sulfur in the thin films.

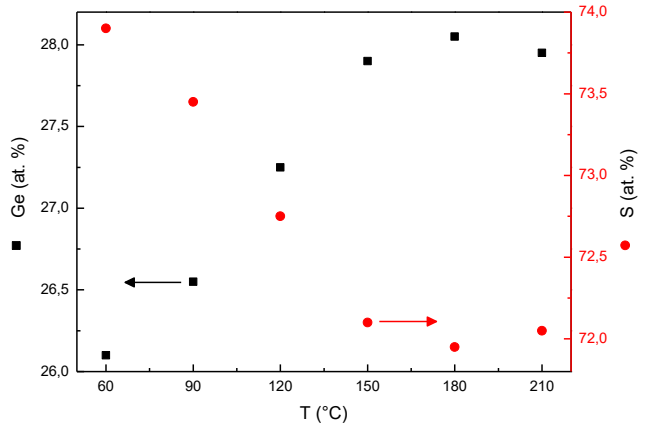

Fig. 7: Dependence of Ge_xS_{100-x} ratio on annealing temperature measured by EDS technique.

The organic molecules content in thin film matrix was investigated using the concentration of nitrogen atoms. The BA molecule contains one nitrogen atom and there is no other possible source of nitrogen in the studied thin films. Thus nitrogen atomic content should be equivalent to the residual organic molecules bonded inside the glass matrix. The nitrogen content is given relative to the content of germanium in Fig. 8 because the amount of germanium remains stable contrary to the sulfur content (Fig. 7). Obtained EDS results show decreasing concentration of organic molecules in the film matrix (Fig. 8) supporting the previously mentioned result (decrease of intensity of absorption band at 2900 cm^{-1} corresponding to $–CH_2–$, $–CH_3$ and $–NH_2$ vibrations) and it is in good agreement with results reported in the literature for As_2S_3 and As_2Se_3 ChGs thin films prepared by spin-coating [15, 24, 25]. The most significant organics content loss occurs during the annealing at the temperatures above 120 °C. Chern and Lauks observed similar trend in case of spin-coated As_2S_3 thin films, but at lower annealing temperature (80 °C) [13]. They proposed that organic molecules bonded in form of alkyl ammonium arsenic sulfide (AAAS) salts start to decompose at 80 °C and further increase of annealing temperature supports decomposition process. Thus, the formation of similar alkyl ammonium germanium sulfide (AAGS) salts can be expected during dissolving of germanium-sulfide ChG in BA, but the AAGS salts probably start to decompose at higher temperatures in comparison with AAAS salts.

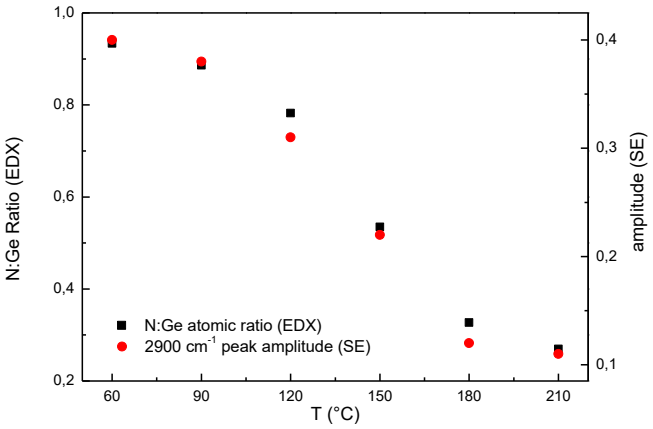

Fig. 8: Dependence of the nitrogen/germanium ratio measured by EDS and the amplitude of 2900 cm^{-1} absorption band in SE data on the temperature of annealing for spin-coated $Ge_{25}S_{75}$ thin films.

Release of organic molecules during the thermal treatment of spin-coated $Ge_{25}S_{75}$ thin films affects also the chemical stability of thin films [20, 21]. In order to investigate the changes in chemical resistance of deposited thin films the samples annealed at various temperatures were etched in 0.1% vol. BA solution in aprotic solvent. The as-prepared thin film and thin films annealed at 90 and 120 °C were dissolved immediately after their immersion into the etching solution. Dissolving of the thin films annealed at and above 150 °C took significantly longer time (tens of seconds and more). Obtained etching curves and calculated etching rates (Fig. 9) proved, that the chemical stability gradually increases with increasing annealing temperature. According to the literature [16, 17] the annealing above the organic salts decomposition temperature also induces significant structural polymerization resulting in more compact thin films. As the organic AAGS salt decomposition temperature was based on SE and EDS measurements expected to be above 120 °C, the chemical stabilization effect of annealing is evident.

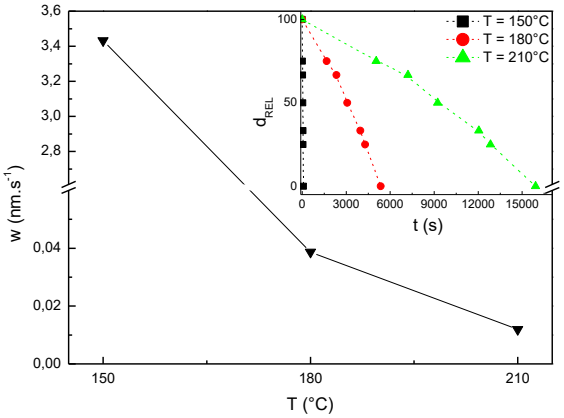

Fig. 9: The annealing temperature dependence of calculated etching rates of studied thin films in 0,1% vol. BA based etching solution. Inset shows the etching curves of $Ge_{25}S_{75}$ spin-coated samples.

To support suggested explanation of annealing induced changes of optical parameters and chemical stability, the Raman spectra of pure BA solvent, source bulk glass and thin film samples were measured (Fig. 10). The main structural units of source bulk $Ge_{25}S_{75}$ ChG are $GeS_{4/2}$ tetrahedra with band at 340 cm^{-1} [35–38]. Two weak bands at 368 and 436 cm^{-1} can be attributed to the vibration of edge-shared $GeS_{4/2}$ tetrahedral structural units [36, 37]. Due to the sulfur overstoichiometry of $Ge_{25}S_{75}$ ChG, three bands at 151, 218 and 475 cm^{-1} are present in measured spectra. These bands can be attributed to the vibrations of S_8 rings [39–41].

The Raman spectrum of as-prepared thin film proved, that its structure is very different from source bulk glass. The main structural units of as-prepared spin-coated thin film are also $GeS_{4/2}$ tetrahedra with band at 340 cm^{-1}, but contrary to the source bulk glass the $GeS_{4/2}$ tetrahedra band is sharp and narrow. The edge-shared $GeS_{4/2}$ tetrahedra bands (368 and 436 cm^{-1}) are not present in the Raman spectrum of as-prepared sample suggesting low level of structural polymerization. The S_8 ring bands at 151, 218 and 475 cm^{-1} are also present in measured spectrum, but their intensity is higher than in the Raman spectrum of source bulk glass. The bands at 2800 – 3000 cm^{-1} prove that the deposited thin films contain also residual BA molecules [16]. Three additional bands at 144, 191 and 455 cm^{-1} can be identified in Raman spectrum of as-prepared sample. These bands are not present in the Raman spectrum of source bulk glass and to our best knowledge they do not correspond to any published vibration of germanium or sulfur compound. The intensity of the bands at 144, 191 and 455 cm^{-1} in Raman spectra of as-prepared and annealed thin films exhibits similar trend as the

annealing temperature dependence of nitrogen content (Fig. 8). The intensity of these bands significantly decreases in Raman spectra of the samples annealed above 120 °C. Thus we can assume that these new bands have connection with organic molecules content and one or more of them can be attributed to the vibrations of proposed alkyl ammonium germanium sulfide (AAGS) salts molecules. Analogously additional band was already reported in the Raman spectra of spin-coated arsenic-sulfur thin films [16, 17] and it was assigned to the vibration of alkyl ammonium arsenic sulfide (AAAS) salts molecules.

The Raman spectra of thin films annealed at 90 °C and 120 °C proved that their structure changes only negligibly. It is with a good agreement with EDS and MIR spectroscopic data, which showed only minor organics content decrease. Contrary, the structure of sample annealed at 150 °C is very different from the structure of as-prepared thin film. The intensities of organic-related bands at 144, 191, 455 and 2800 – 3000 cm^{-1} are significantly reduced. The edge-shared $GeS_{4/2}$ tetrahedra bands at 368 and 436 cm^{-1} are also present in measured spectrum suggesting structural polymerization. The Raman spectrum of thin film annealed at 180 °C is almost identical with the spectrum of source bulk glass. The AAGS salts molecules are decomposed and the S_8 rings are almost completely dissolved into the glass matrix. Unfortunately the luminescence is present in Raman spectra of the samples annealed at and above 150 °C. The intensity of the luminescence significantly overlaps the intensity of Raman signal in case of thin film annealed at 210 °C.

Similarly to the arsenic-sulfur spin-coated thin films [13–17], the Raman spectra of spin-coated $Ge_{25}S_{75}$ samples confirmed thermo-induced structural polymerization connected with decomposition of AAGS salts and releasing the organic molecules. It results in changing of the thin films structure close to the structure of the source bulk glass.

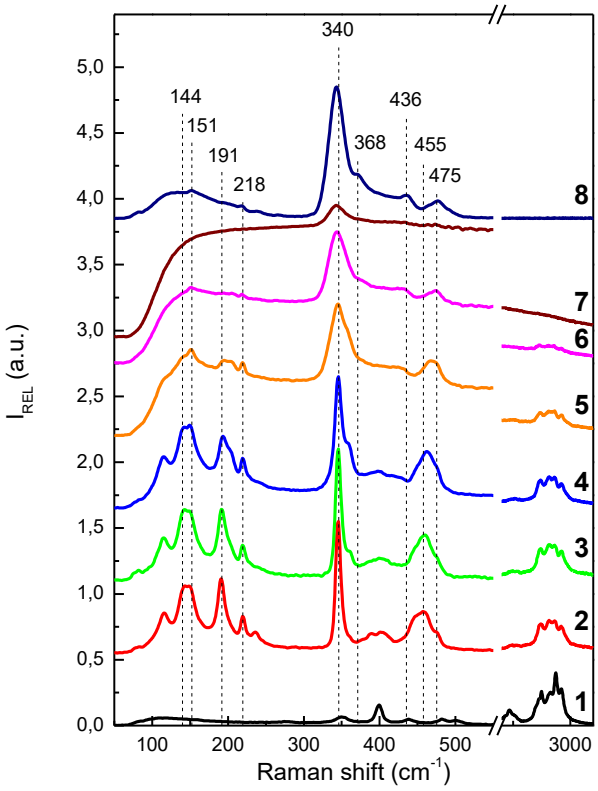

Fig. 10: The Raman spectra of pure BA solvent, source bulk glass and annealed spin-coated $Ge_{25}S_{75}$ thin film samples. 1 – pure BA solvent, 2 – as-prepared thin film, 3 – annealed at 90 °C, 4 – annealed at 120 °C, 5 – annealed at 150 °C, 6 – annealed at 180 °C, 7 – annealed at 210 °C, 8 – source bulk glass.

4. Conclusion

We report on the investigation of the structure and properties of non-toxic amorphous chalcogenide $Ge_{25}S_{75}$ thin films prepared by spin-coating technique. Influence of annealing temperature on structure, composition, optical and chemical properties have been studied.

Optical properties of as-prepared sample and samples annealed at different temperatures have been studied by SE in wide spectral range (0.05 – 6 eV). Deposited thin films are transparent up to ≈ 20 μm in the MIR part of spectra. Absorptions bands in MIR part of spectra were assigned to vibrations of organic residues. The refractive index in the transparent spectral region is increasing and the values of optical band gap are decreasing with increasing annealing temperature. These facts correspond to the increase of the layer compactness manifested by significant decrease of film's thickness with the increasing annealing temperature.

Based on the EDS and Raman spectroscopy measurements most of organic residues decompose and evaporate during the annealing at temperatures higher than 120 °C. Annealing temperature above 150 °C is sufficient to obtain chemically stable spin-coated thin films with structure close to the source bulk glass. Thermally induced structural polymerization connected with decomposition of alkyl ammonium germanium sulfide (AAGS) salts and releasing organic molecules is proposed as probable mechanism of annealing induced changes of structure and properties of spin-coated $Ge_{25}S_{75}$ chalcogenide thin films.

Acknowledgement

Authors appreciate financial support from project No. 16-13876S financed by the Grant Agency of the Czech Republic (GA CR) as well as support from the grants LM2015082 and CZ.1.05/4.1.00/11.0251 from the Ministry of Education, Youth and Sports of the Czech Republic.